Available online at www.sciencedirect.com
SCIENCE DIRECT
Journal of Power Sources 146 (2005) 190–194
JOURNAL OF POWER SOURCES
www.elsevier.com/locate/jpowsour

Lithium insertion in Si–TiC nanocomposite materials produced by high-energy mechanical milling

Z.P. Guo *, Z.W. Zhao, H.K. Liu, S.X. Dou

Institute for Superconducting and Electronic Materials, University of Wollongong, Wollongong, NSW 2522, Australia

Available online 25 May 2005

Abstract

Silicon and titanium carbide (TiC) nanocomposites were synthesized using a high-energy ball-milling technique. X-ray diffraction analyses show that the nanocomposite consists of amorphous silicon and nanocrystalline titanium carbide. The electrochemically inactive TiC working as a buffer matrix successfully prevents Si from cracking/crumbling during the charging/discharging process. The nanocomposite containing 40 mol% silicon obtained after milling for 4 h exhibits a stable capacity of ~380 mAh g^{-1}, suggesting its promising nature in anode materials for the lithium ion battery.

Keywords: Nanocomposites; Silicon; Titanium carbide; Anode; Lithium-ion batteries

1. Introduction

Lithium-ion batteries using a graphite- or coke-based carbon anode have rapidly become important for use in a variety of electronic devices. In spite of their successful commercialisation, however, various new anode materials are being investigated to overcome the limited capacity of graphite (372 mAh g^{-1}). Attention has been paid to lithium alloys, such as Sn and Al alloys, which give theoretical capacities from 990 to 1000 mAh g^{-1} [1–4]. The highest capacity is perhaps from Li–Si alloys where a high Li/Si stoichiometry (4.4:1) and the low atomic weight of Si combine to give capacities around 4000 mAh g^{-1} [5]. Unfortunately, there is one severe problem with most lithium alloy anodes, i.e., the large volume change during lithium intercalation/de-intercalation, which inevitably pulverizes the alloy particles. The resulting loss of connectivity with the conducting additive particles causes poor cyclability in practice [6].

A popular approach to counter particle pulverization is to reduce the Si particle size to give a small absolute volume change in the local environment. Alternatively, the active particles may be embedded in a less active or inactive matrix to cushion the expansion and contraction in charge and discharge reactions. Recently, Dahn and co-workers have reported a Sn–Fe–C-based nanocomposite, consisting of active Sn_2Fe and almost inactive $SnFe_3C$ [4,7]. Thackeray and co-workers also demonstrated the potential of the Cu_6Sn_5, InSb and MnSb systems [8–10]. Other active–inactive composite systems such as Si–TiN and Si–TiB_2 have also been studied [11,12]. Although these systems are promising, there are problems related to long processing time, irreversible loss, capacity and/or cyclability. Therefore, it is necessary to further improve the demonstrated concept of active–inactive composites.

The purpose of this paper is to improve the active–inactive concept further by exploring silicon/titanium carbide (Si/TiC) composite as an anode material. The Si/TiC nanocomposites were synthesized by high-energy mechanical milling. The process results in very fine or amorphous silicon particles distributed homogeneously inside the TiC matrix.

* Corresponding author. Fax: +61 2 4221 5731.
E-mail address: zguo@uow.edu.au (Z.P. Guo).

0378-7753/$ – see front matter © 2005 Elsevier B.V. All rights reserved.
doi:10.1016/j.jpowsour.2005.03.113

2. Experimental

2.1. Materials preparations

Nanocomposites of Si and TiC were prepared using a Retsch MM301 high-energy mechanical mill. Commercially obtained elemental powders of Si (average size: <100 nm) and TiC (average size: 80 nm) were used as starting materials. Stoichiometric amounts of the powders were weighed and loaded into a hardened steel vial containing hardened steel balls inside an argon-filled glove box. The vial was firmly sealed to prevent and minimize any oxidation of the starting materials.

2.2. Electrochemical tests

A 1-methyl-2-pyrrolidone (NMP) slurry of 85 wt.% composites, 10 wt.% carbon black and 5 wt.% poly(vinylidene fluoride) (PVDF) was used to coat 20 μm copper disks to a mass loading of 1–2 mg cm^{-2} after drying (at 100 °C) and compaction (at 2.0×10^6 Pa). Each coated electrode was assembled into a test cell using a Li counter electrode, a Celgard 2500 separator, and an electrolyte of 1 M $LiPF_6$ solution in a 50:50 mixture of ethylene carbonate (EC) and diethyl carbonate (DEC). The assembly was carried out in an argon-filled glove box with less than 1 ppm each of oxygen and moisture. The cells were charged and discharged at room temperature between 0.02 and 1.2 V at a constant current density of 0.25 mA cm^{-2} on a cell tester.

2.3. Materials characterizations

The phases present in the as-milled powders and the cycled electrode were analysed using a scanning electron microscope and X-ray diffraction. The SEM observation was performed on a Leica scanning electron microscope. The X-ray diffraction was carried out by using a Philips 1730 diffractometer with Cu Kα radiation.

3. Results and discussion

In the current study, nanocomposites of Si and TiC were prepared using a Retsch MM301 high-energy mechanical mill. Kumta and co-workers [11,12] reported that Si/TiN and Si/TiB_2 were synthesized using a SPEX-8000 high-energy ball-mill. To obtain a stable capacity, the ball-milling time had to be more than 15 h. However, in this work, Si/TiC nanocomposite composed of amorphous Si and nanocrystalline TiC can be obtained by milling Si and TiC for only 4 h. By varying the ball-milling parameters (shaking frequency, ball to powder mass ratio and duration of milling), it was found that the microstructure of the ball-milled nanocomposites depends strongly on the shaking frequency. The optimal shaking frequency with respect to phase composition, microstructure and contaminations was found to be 25 Hz. Fig. 1

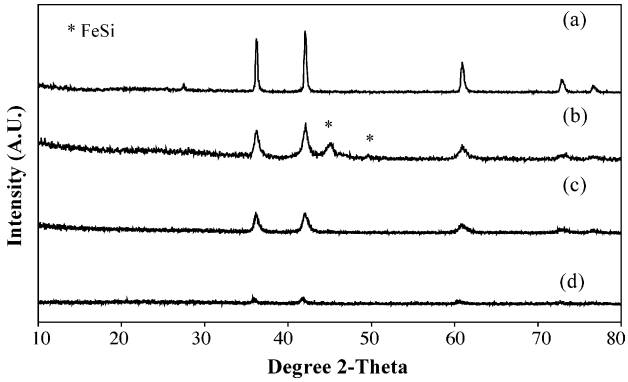

Fig. 1. XRD patterns of (a) TiC; (b) Si:TiC = 2:3 nanocomposites milled at a frequency of 30 Hz for 1 h; (c) Si:TiC = 2:3 milled at a frequency of 25 Hz for 4 h; and (d) Si:TiC = 2:3 milled at a frequency of 25 Hz for 8 h.

shows the XRD patterns of the as-milled powders obtained after milling under various conditions. Contamination with iron (FeSi) is found in the sample ball-milled at an higher frequency (30 Hz). With increased ball-milling time, a noticeable broadening of the Bragg peaks is observed, which indicates that a nanocrystalline/amorphous microstructure of the end products has been formed. All peaks in Fig. 1c and d correspond to TiC, while the absence of Si-related peaks in the XRD pattern indicates that Si exists in a nanocrystalline-amorphous form uniformly dispersed in the powder. The effective crystal size, estimated by Scherrer's method from the full width at half maximum of the peak for the TiC as a function of the milling time is presented in Fig. 2. The crystallites were in the 5–10 nm range, and with increased milling time, the crystal size of TiC decreases. Peak broadening due to residual internal strain was not accounted for, and hence the actual size of the crystallites can be expected to be bigger. SEM analysis was conducted on the Si–TiC nanocomposite containing 40 mol% Si after milling for 1 and 4 h to analyse the microstructure (Fig. 3). Fig. 3a shows a SEM micrograph of the nanocomposite obtained after milling for 4 h. It can be seen that the agglomerates are porous and composed of

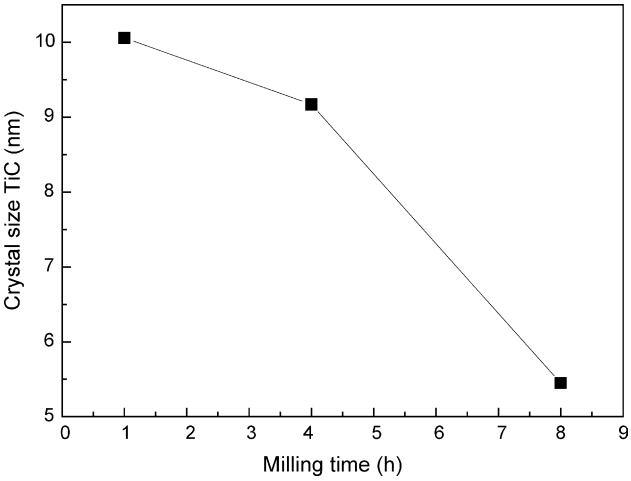

Fig. 2. Evolution of the average grain size of the TiC with the milling time.

small particles. EDX mapping of the different elements was conducted to analyse the distribution of the species within the agglomerated particles (Fig. 3b and c). The bright spots correspond to the presence of each element. Based on the EDX elemental maps, Si and Ti in the sample after milling for 1 h are not completely well distributed, while both Si and Ti are homogeneously distributed in the powder mixture after milling for 4 h. These indicate that a uniform distribution of

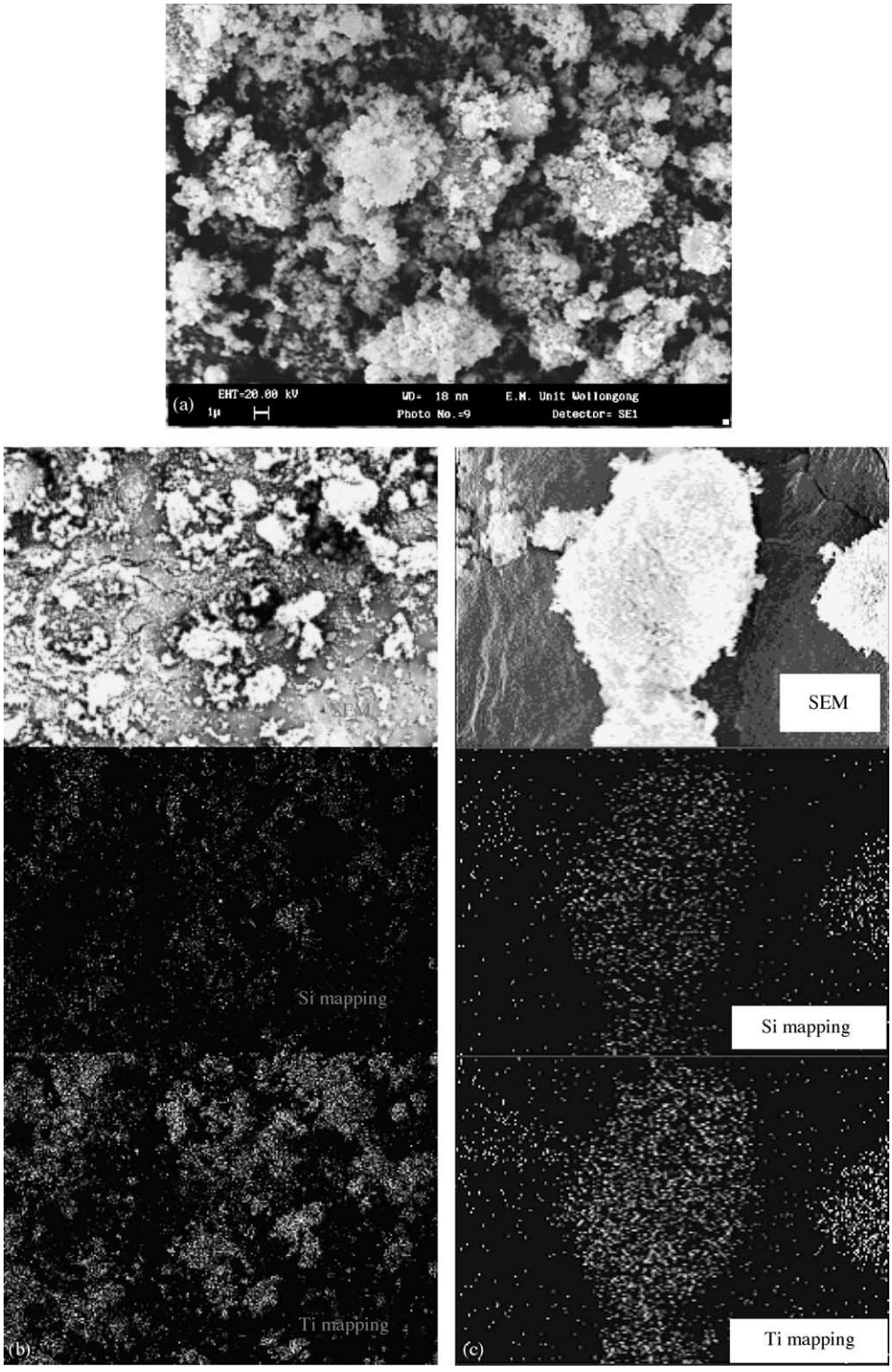

Fig. 3. (a) SEM micrograph of the Si:TiC = 2:3 nanocomposite obtained after milling for 4 h. (b) SEM micrograph and chemcial map of Si and Ti for the Si:TiC = 2:3 nanocomposite obtained after milling for 1 h. (c) SEM micrograph and chemical map of Si and Ti for the Si:TiC = 2:3 nanocomposite obtaining after milling for 4 h.

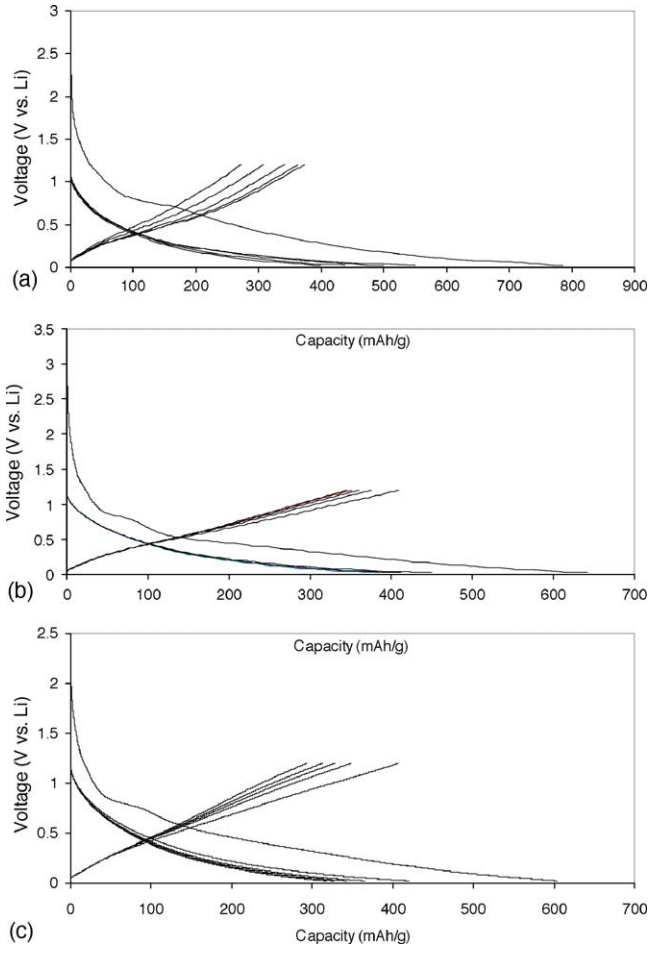

Fig. 4. The charging/discharging curves for the Si:TiC = 2:3 nanocomposites obtained after milling for (a) 1 h; (b) 4 h and (c) 8 h.

Si and TiC within all the particles cannot be achieved after milling for 1 h, but 4 h ball-milling is long enough to obtain a uniformly distributed Si–TiC nanocomposite.

The charging and discharging curves for the nanocomposite containing 40 mol% Si obtained after milling for different times are shown in Fig. 4. A smooth plateau in the low-voltage range without any significant fade in capacity was observed. The first irreversible capacity loss is ∼30% mainly due to the formation of a Li-containing passivation layer and/or possible oxidation of the surface of the composite [13]. It should be noted that the charge/discharge efficiency for the sample after milling for 1 h is lower than for the long ball-milled sample because the Si particles are not homogeneously distributed within the electrochemically inactive but strongly electrically conductive TiC matrix. This result is consistent with the SEM images above. The specific capacity of an electrode prepared with these powders is shown in Fig. 5. The initial capacity appears to decrease as the milling time increases, indicating a reduction in the amount of the active Si phase [11,12]. A possible reason for this could be that the Si nanoparticles are surrounded or covered by TiC, thereby preventing their reaction with lithium. The composite obtained after milling for 1 h shows capacity fade whereas the samples milled for

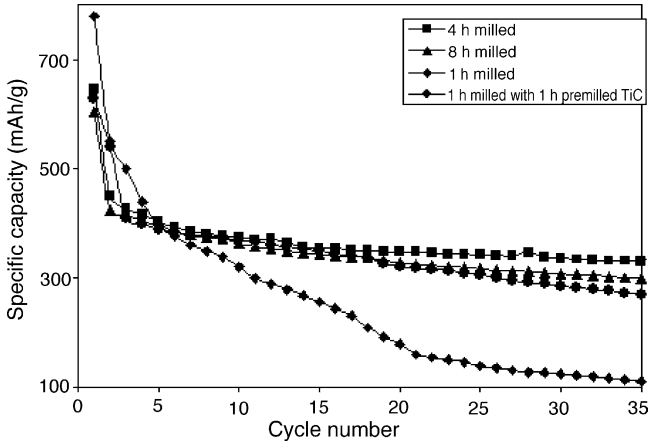

Fig. 5. Capacity as a function of cycle number for the Si:TiC = 2:3 nanocomposites obtained after milling for 1, 4, 8 h and 1h milling with 1 h premilled TiC, respectively.

4 and 8 h exhibit good capacity retention. By carefully comparing the charge/discharge curves of composites obtained after milling for 4 h with those milled for 8 h, it was found the capacity retention of a 4 h sample is even better than that of a sample milled for 8 h. The reason for this could be a possible welding effect between crystallites during the long ball-milling process [14]. The welding effect between TiC and TiC or Si would destroy the matrix to some extent, preventing it from buffering the volume change of the Si crystallites during charge/discharge cycles and thereby slightly decreasing the cyclibility of the Si–TiC electrode.

It has been found that the premilling of a large amount of inactive component (TiB_2) has a good effect on the capacity fading of Si/TiB_2 nanocomposites [12]. What is the premilling effect on the Si/TiC system? The Si/TiC nanocomposite anodes obtained by milling commercial Si powder and 1 h premilled TiC powder mixture for 1 h were tested. The discharge capacity of such an anode varies with cycle number is shown in Fig. 5. The premilled sample shows good capacity retention, which is much better than that of the 1 h milled sample without TiC premilling. This result confirms the conclusion proposed by Kim et al. [12], i.e., a smaller particle size of the inactive component provides better volume change buffer capability because the stress induced by volume expansion of the active phase during cycling is distributed more homogeneously in the composite containing inactive component with smaller particle size.

To directly analyse any changes in the microstructure or morphology of the particles during cycling, the electrodes fabricated from the composites containing 40 mol% Si obtained after milling for 4 h were observed before and after cycling with SEM. Fig. 6a is a SEM image showing the surface of the Si–TiC electrode before cycling and Fig. 6b is the SEM micrograph of the electrode after 30 cycles. There appears to be no change in the morphology of the particles before and after cycling, suggesting good structural stability of the nanocomposite. This excellent stability of the electrode may be attributed to the existence of very finely dispersed Si

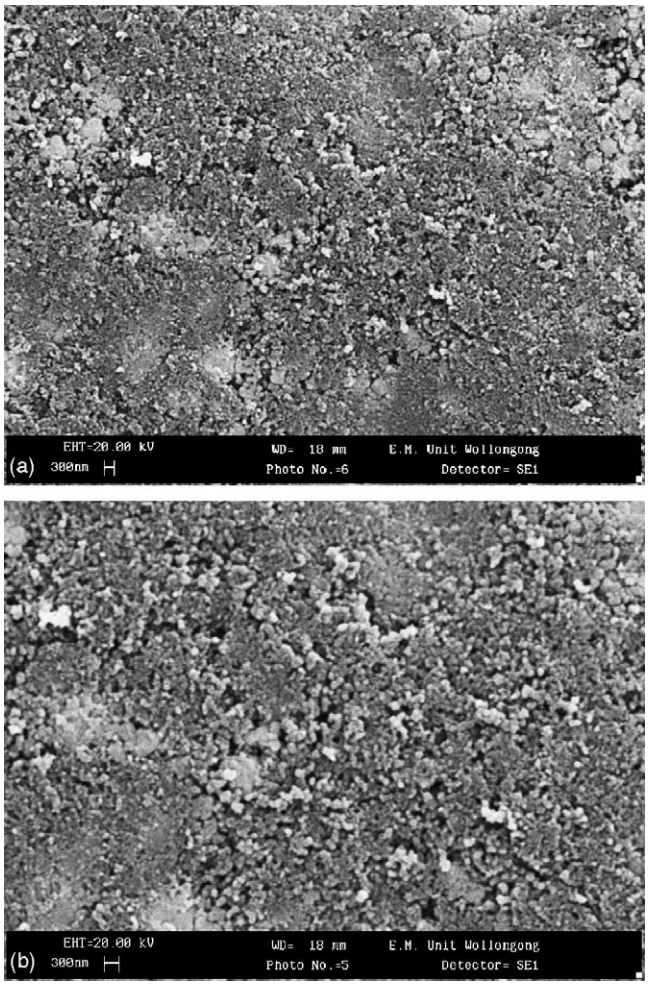

Fig. 6. SEM images of the electrode (a) before and (b) after 30 cycles.

particles within the TiC matrix. The Si reacts with lithium reversibly without undergoing any noticeable particle growth. This suggests that TiC could be a very good inactive matrix for Li-ion anodes.

4. Conclusion

Si–TiC nanocomposite composed of amorphous Si and nanocrystalline TiC can be obtained by milling Si and TiC for only 4 h. As the milling time was increased, a reduction in the initial specific capacity was observed, prolonged milling appears to cause an increase in the inactive portion of Si. The as-prepared powder consists of agglomerates of nanosized particles. The cyclic performance of the Si anode is improved, because TiC works as a buffering environment to prevent Si from cracking/crumbling during charge/discharge cycles. Premilling of the inactive TiC component could improve the buffer effect of TiC and increase the stability of the capacity of the Si/TiC nanocomposite electrodes.

Acknowledgements

Financial support provided by the Australian Research Council (ARC), Sons of Gwalia Ltd., OM Group and Lexel Battery Ltd. are gratefully acknowledged.

References

[1] M. Winter, J.O. Besenhard, Electrochim. Acta 45 (1999) 31.
[2] Sanyo Electric, U.S. Patent 4,820,599 (1989).
[3] B.A. Boukamp, G.C. Lesh, R.A. Huggins, J. Electrochem. Soc. 128 (1981) 725.
[4] O. Mao, J.R. Dahn, J. Electrochem. Soc. 146 (1999) 405.
[5] R.A. Sharma, R.N. Seefurth, J. Electrochem. Soc. 123 (1976) 1763.
[6] R.A. Huggins, Solid State Ionics 113–115 (1998) 57.
[7] O. Mao, R.L. Turner, I.A. Courtney, B.D. Fredericksen, M.I. Buckett, L.J. Krause, J.R. Dahn, Electrochem. Solid State Lett. 2 (1999) 3.
[8] K.D. Kepler, J.T. Vaughey, M.M. Thackeray, Electrochem. Solid State Lett. 2 (1999) 307.
[9] J.T. Vaughey, J. O'Hara, M.M. Thackeray, Electrochem. Solid State Lett. 3 (2000) 13.
[10] L.M.L. Fransson, J.T. Vaughey, K. Edstrom, M.M. Thackeray, J. Electrochem. Soc. 150 (2003) A86.
[11] S. Kim II, P.N. Kumta, G.E. Blomgren, Electrochem. Solid State Lett. 3 (2000) 493.
[12] S. Kim II, G.E. Blomgren, P.N. Kumta, Electrochem. Solid State Lett. 6 (2003) A157.
[13] K.-C. Moller, H.J. Santner, W. Kern, S. Yamaguchi, J.O. Besenhard, M. Winter, J. Power Sources 119–121 (2003) 561.
[14] T. Spassov, P. Solsona, S. Surinach, M.D. Baro, J. Alloys Compd. 349 (2003) 242.